Journal of Materials and Environmental Sciences
ISSN : 2028-2508
CODEN : JMESCN

J. Mater. Environ. Sci., 2018, Volume 9, Issue 8, Page 2263-2273

http://www.jmaterenvironsci.com

Mineralogy and firing characteristics of clayey materials used for ceramic purposes from Sale region (Morocco).

M. El Halim [1,2*], L. Daoudi [1], M. El Ouahabi [2], J. Amakrane [2,3], N. Fagel [2]

[1]*Laboratoire de Géosciences et Environnement (LGSE), Département de Géologie, Faculté des Sciences et Techniques, Université Cadi Ayyad, BP 549 Marrakech, Morocco*

[2]*UR Argile, Géochimie et Environnement sédimentaires (AGEs), Département de Géologie, Quartier Agora, Bâtiment B18, Allée du six Août, 14, Sart-Tilman, Université de Liège, B-4000, Belgium*

[3]*Laboratoire des géosciences appliquées (LGA), Département de Géologie, Faculté des Sciences, Université Mohammed Premier, BP 717 Oujda, Morocco*

Received 21 Oct 2017,
Revised 14 Dec 2017,
Accepted 17 Dec 2017

Keywords

- ✓ *Clayey material,*
- ✓ *Ceramics,*
- ✓ *Characterization,*
- ✓ *Sale,*
- ✓ *Morocco.*

elhalim.mouhsin@gmail.com
Phone: +212627008488;
Fax: +212528800399

Abstract

Clayey marls from the Bouregreg basin (Morocco) used traditionally in the ceramic industry of Sale were studied by mineralogical and physico-chemical characterization in order to evaluate their potential suitability as raw materials in ceramic applications. X-ray diffraction (XRD) and Fourier Transform-Infrared (FT-IR) spectrometry are used to establish the mineralogical composition. Physical properties were identified by particle size distribution and consistency limits. Chemical composition was carried out by XRF technique. The clay suitability for traditional ceramics was discussed in view of its granulometric distribution, plasticity and thermal behavior. Two clay materials, 75% of upper Miocene marl (ARSNS) and 25% of Triassic clay (ARSNI), are used for the manufacture of utility ceramics in Sale region, the first rich in carbonates (20% of CaO) and the second non-calcareous. The chemical compositions indicated that SiO_2, Al_2O_3 and Fe_2O_3 are major elements while K_2O and MgO are less abundant. Quartz, Feldspar and clay minerals prevail in all samples, with kaolinite, illite and smectite being the dominant phases. The classification of these samples using appropriate ternary diagrams showed that the proportions used in the mixture lead to a new material (ARSM) with adequate characteristics for the production of traditional ceramics.

1. Introduction

The oldest method of making terracotta objects is by using only hands and clay. This technique is still used today. After the pottery has been formed and dried completely, it must be cooked to get a hard and tight material. Without the chemical transformation that occurs during cooking, an uncooked piece dissolves in contact with water. The usual cooking is done in gas, coal or wood ovens. Mineral modifications and the final characteristics of heated piece are influenced mainly by the chemical and mineralogical compositions of the raw materials, the maximum heating temperature, the heating rate, the duration of firing, and the kiln redox atmosphere. Thus, the maximum temperature in an oven is often kept constant for a period of time to ensure the required maturity in terracotta.

In Morocco, pottery is recognized internationally by its artistic specificity according to the regions. The five production centers of Moroccan pottery are: Fez, Safi, Sale, Marrakech and Tetouan. However, traditional methods of producing traditional ceramics, which do not take into account chemical and mineralogical characteristics, are still practiced in these centers. Actually, with the exception of some recent studies which mainly concern the clays of Tetouan, Meknes and Tangier [1-2], the clays of Fez [3] and the clays of the Marrakech region [4-6], very limited studies have been carried out on the quality and potential use of Moroccan clays in the manufacture of ceramic objects in the Sale site.

This study focuses on mineralogical, chemical and geotechnical characterization of the raw clay materials used by potters in Sale (West Morocco) for the manufacture of terracotta objects. The exceptional plasticity of the surrounding clay soil has built the popularity of the traditional ceramics of Sale. However, the potters in the complex of Sale (Oulja) try always to explore materials whose mineralogically and geotechnically are the most adequate to maintain the specificity of Slaouite ceramics.

2. Material and Methods

2.1. Materials

The potters site of Oulja is located on the Bouregreg river at 10 km from the center of Rabat (Figure 1). From a geological point of view, the Rabat-Sale region is characterized by outcrops of the Palaeozoic basement at the edges of the great rivers of the region with a large post Palaeozoic cover locally very thick [7], which offers a variety of petrographic facies, some of them have the value of geomaterials highly sought by the ceramic industry. Oulja's potters use a mixture of two main materials for the manufacture of utility ceramics: upper Miocene yellow marls (ARSNS), with extensive layers in the whole region, and Triassic clay (ARSNI) represented as a deposit whose thickness doesn't exceeds tens of meters. These two materials were prepared by traditional methods, mixed by feet and cooked in traditional wood-burning ovens.

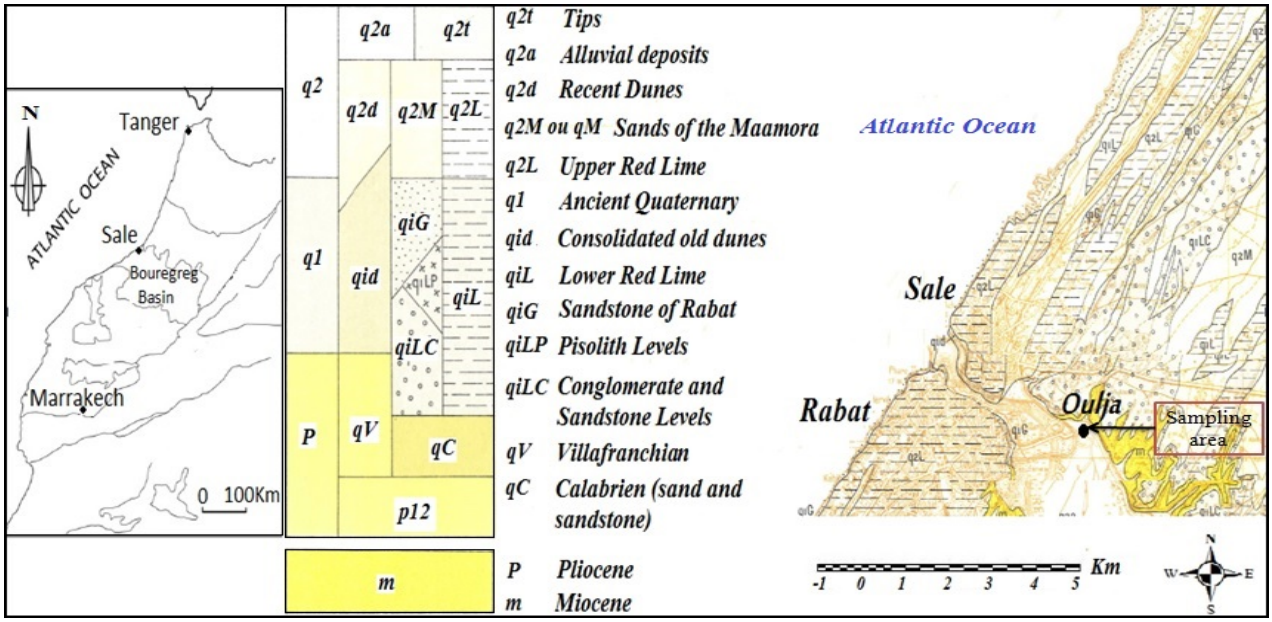

Figure 1: Geological map of the Rabat-Sale region and geographical location of the Oulja pottery complex [8].

The artisans of Oulja use the turning process which consists in revolving a mass of the dough resulting from the mixture of ARSNS and ARSNI on a rotary axis. Water is essential in this stage to make the shaping of the dough more practical (Figure 2).

Figure 2: Village of potters in Oulja, Process of turning (A) and the enamelled finished product (B).

Finished piece is placed outside for a slow drying towards one to two days depending on the climate. Once dried, the piece is introduced into a traditional oven for a first cooking; the cooking temperature in these ovens

is estimated at 900°C. The enamelling of the part is done by a glaze mixture based on lead, and it is introduced again into the furnace for a second firing, the heat treatment cycle is identical to that of the first firing.
The three types of samples that have been characterized in this study are: 1) a sample of Triassic Oulja clays (ARSNI) whose contribution to the mixture did not exceed 25%, 2) a sample of the upper Miocene marls (ARSNS) which constitute about 75% of the ceramic paste (Figure 3), and a mixture sample of these two materials (ARSM) ready to be used in the preparation of decorative ceramics. These samples were taken directly from the Oulja site.

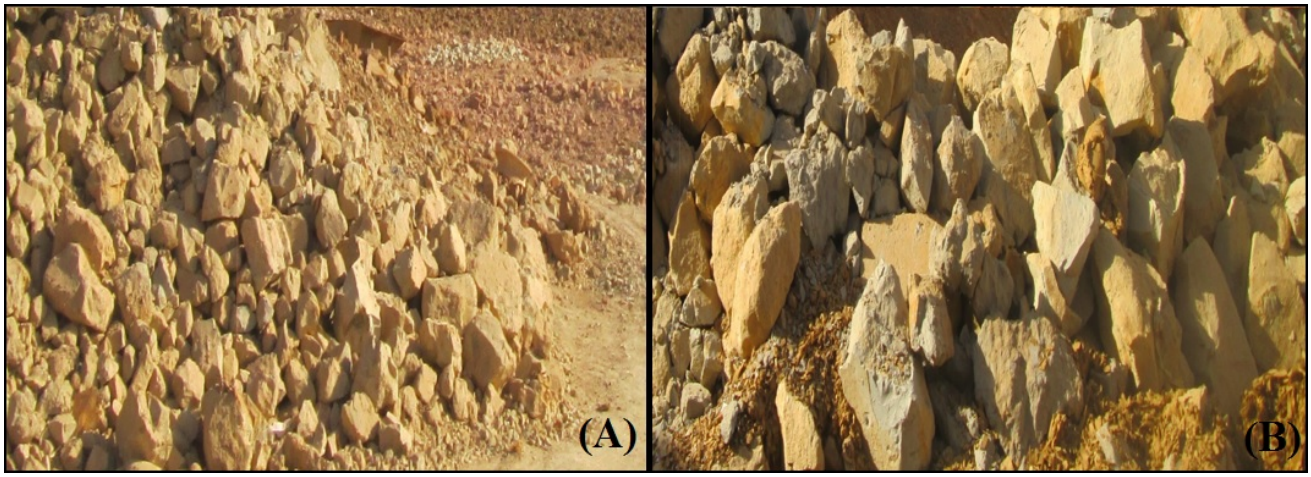

Figure 3: The raw materials (A) ARSNS and (B) ARSNI used by artisans in the pottery of Sale.

2.2. Methods

The clay materials were sorted to provide statistically valid samples. Firstly, all samples were dried at 40°C for 48 h, and then characterized by X-ray diffraction (XRD), Infrared Spectroscopy (FTIR), particle size distribution, X-ray fluorescence chemical analysis (XRF), Thermal evolution and plasticity measurement.
The mineralogical composition was identified by X-ray diffraction using a Bruker D8 Advance powder diffractometer with copper anticathode CuKα (ƛ = 1.5418 Å), bound to a high voltage generator (40 kV, MA, 1200 W) and coupled with EVA software. The lines of the obtained diffractograms are allocated by comparison with the data of the A.S.T.M (American Society for Testing and Materials). The clay fraction was recerded sequentially under natural or dehydrated conditions in air (N), after salvation with ethylene glycol for 24 h (EG) and after heating at 500°C for 4 h (H). A semi-quantitative analysis was performed accordin to [9] for total mineralization and clay fraction with an estimated uncertainty of ± 5%.
The infrared spectra (IRTF) were performed using a NICOLET NEXUS Fourier transform spectrophotometer in the wavelength range of 400 cm^{-1} to 4000 cm^{-1}, the spectral resolution is 1 in the order of 4 cm^{-1}. The samples were diluted in a KBr matrix in proportions of 1 to 2 mg of clay material per 150 mg of KBr before analysis.
The particle size distribution of the samples was measured on bulk sediment using a Malvern Mastersizer 2000 laser diffraction particle analyser coupled to a HydroS wet dispersion unit with a 2000 rmp stirrer. The samples were introduced into 100 ml of deionized water and then placed on a magnetic stirrer to remove any agglomerates. For a complete analysis, three measurements were taken for each sample. The clay fraction was estimated by tests of methylene blue according to the standard NF P94-068 [10] and confirmed by the laser granulometry.
Chemical analysis of the major elements was carried out by X-ray fluorescence spectroscopy (XRF) using a Panalytical Axios spectrometer equipped with Rh tube, the gas used is argon / methane. In order to determine the loss on ignition (LOI), the samples were heated to 1000°C in the furnace for 2 hours.
Plasticity was obtained by determining Atterberg limits: liquid limit (IL), plastic limit (PL) and plasticity index (PI). The plasticity index was calculated by the difference between the LL and PL of the studied samples. These tests were carried out with a Casagrande apparatus according to standard NF P94-051 [11].
Clay samples were dried at 105°C for 24 h and kiln-fired at different temperatures (500, 600, 700, 800, 900, 1000 and 1100 °C) over 4 h. The mineralogical identification and thermal evolution were followed by X-ray diffraction. The samples used for the water absorption and weight loss tests were 5 cm long, 2 cm wide and 2 cm thick. These pieces were fired at different temperatures from 500 °C to 1100 °C, and weighed (P1), then immersed in clean water at 25 °C for 24 hours. The obtained weight (P2) of each specimen was measured immediately after they were removed from water. Water Absorption Capacity was calculated as WAC = (P2 - P1) / P1 × 100% according to standard procedure UNE 67-027 [12].

3. Results and discussion

3.1. Characterization of samples

3.1.1. Particle distribution

The results of granulometric analysis show a little variation in particle size (Figure 4A), with clay fraction (<2 µm) ranges from 24.4 to 35.8%, silt fraction from 64.1 to 71%, and sand fraction from 0.1 to 9.1% (Table 1). The data collected from the particle size analysis of these samples were projected in the McManus ternary diagram [13] (Figure 4B).

Table 1: Particle size distribution, consistency limits (%) and Methylene blue value of the studied samples.

Physical properties	ARSNI	ARSNS	ARSM
Particle size distribution (%)			
Clay (<2 µm)	35.8	24.4	25.5
Silt (2–60 µm)	64.1	66.4	71
Sand (>60 µm)	0.1	9.1	3.5
Consistency limits (%)			
Liquid limit	68.9	44.8	55.6
Plastic limit	29.1	22.8	28.3
Plasticity index	39.7	21.9	27.3
methylene blue VBS	15	6	6

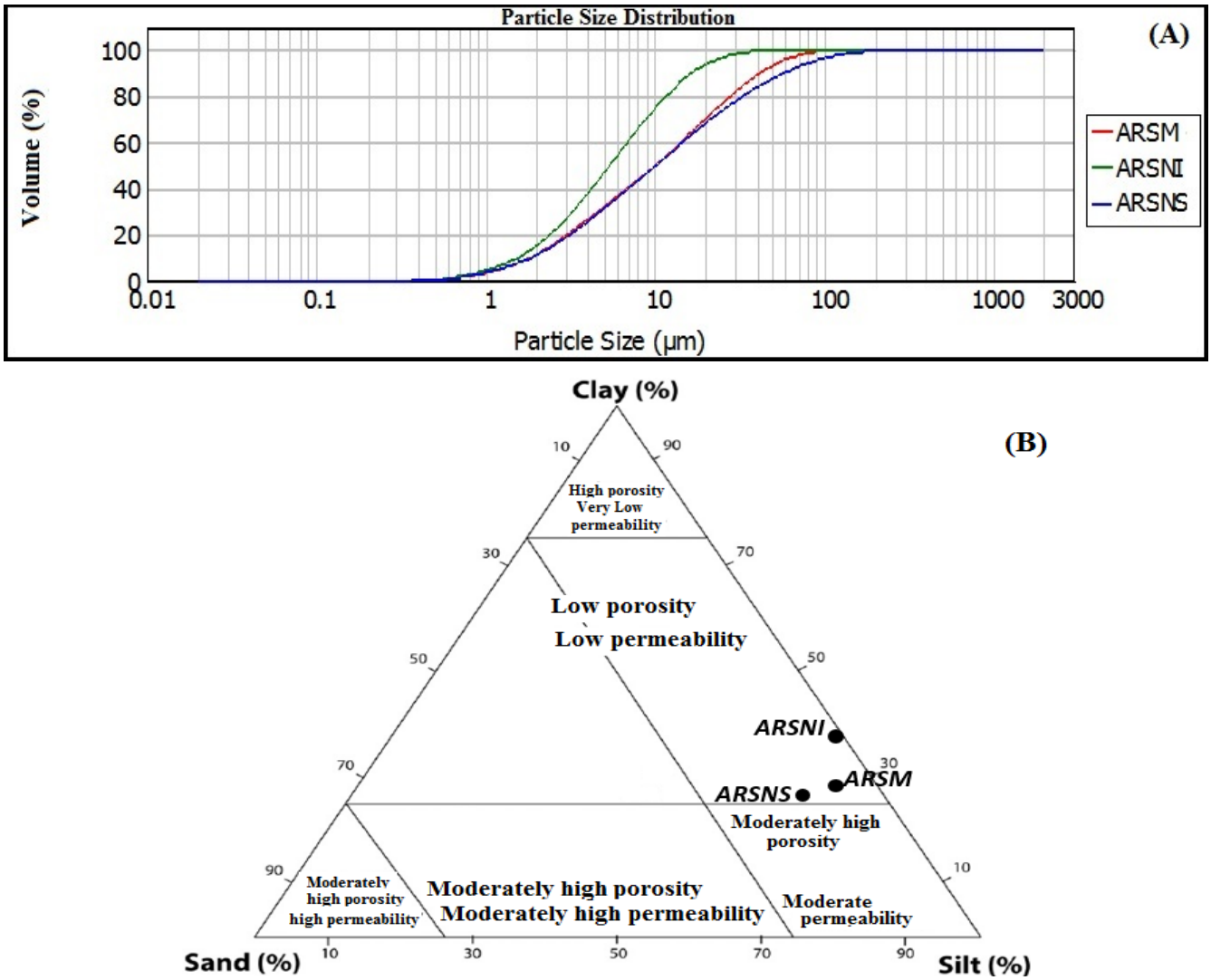

Figure 4: (A) Particle size distribution curves, **(B)** Ternary diagram of the studied soil samples according to [12].

This diagram depends on the relationship between the three sand, silt and clay components and their impacts on porosity and soil permeability. The studied samples are placed in the zone of low porosity and permeability due to their high silts and clay contents. The ARSNS sample came close to the area of moderately high porosity and permeability due to its moderate sand fraction content. The activity of the clay fraction, determined by the ratio between the value of methylene blue VBS and the content of particles smaller than 2 µm, according to standard NF P94-057 [14], shows that this fraction is very active in the ARSNI sample which has a VBS value equal to 15. Whereas for the other samples (ARSNS and ARSM) the clay fraction is moderately active and the VBS value is 6.

3.1.2. Mineralogical Composition

The X-ray diffraction patterns (DRX) of the clay fraction studied on oriented (normal, glycolate and heated to 500°C) blade show that the ARSNI sample contains 25% of illite, 16% of smectite and 8% of kaolinite which appear under the effect of Ethylene glycol at 10.1 Å, 17.1 Å and 7.1 Å, and respectively (Figure 5A). In addition to 12% of illite, 4% of smectite, 5% of kaolinite, the ARSNS sample contains a small amount of chlorite (2%), which appears in the glycol slides at 14 Å (Figure 5B).

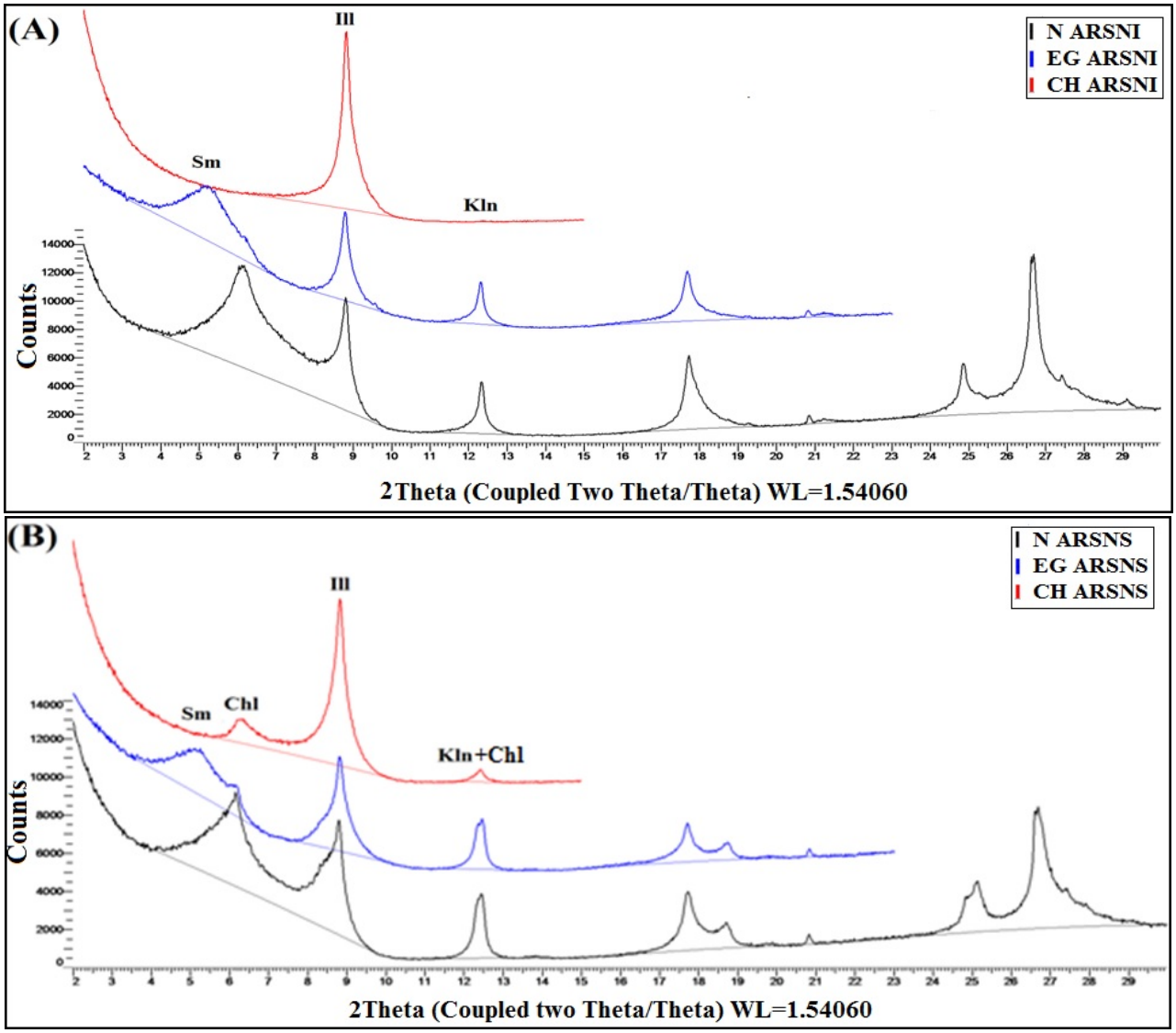

Figure 5: DRX diffractograms of oriented clay blades (normal blade (N), glycol blade (EG) and blade heated to 500°C) of the ARSNI (A) and ARSNS (B) samples. With, Kln: Kaolinite, Ill: Illite, Chl: Chlorite and Sm: Smectite.

The mineralogical composition of the two samples shows the abundance of quartz (22-30%) with moderate feldspar contents (9-12%). The ARSNS sample is rich in carbonates, the calcite content is about 33% and the

dolomite is present at 3%, while ARSNI contains only about 1% calcite (Figure 6). The content of quartz, calcite, dolomite, and feldspars in the ARSM mixture is 31%, 17%, 2% and 14%, respectively.

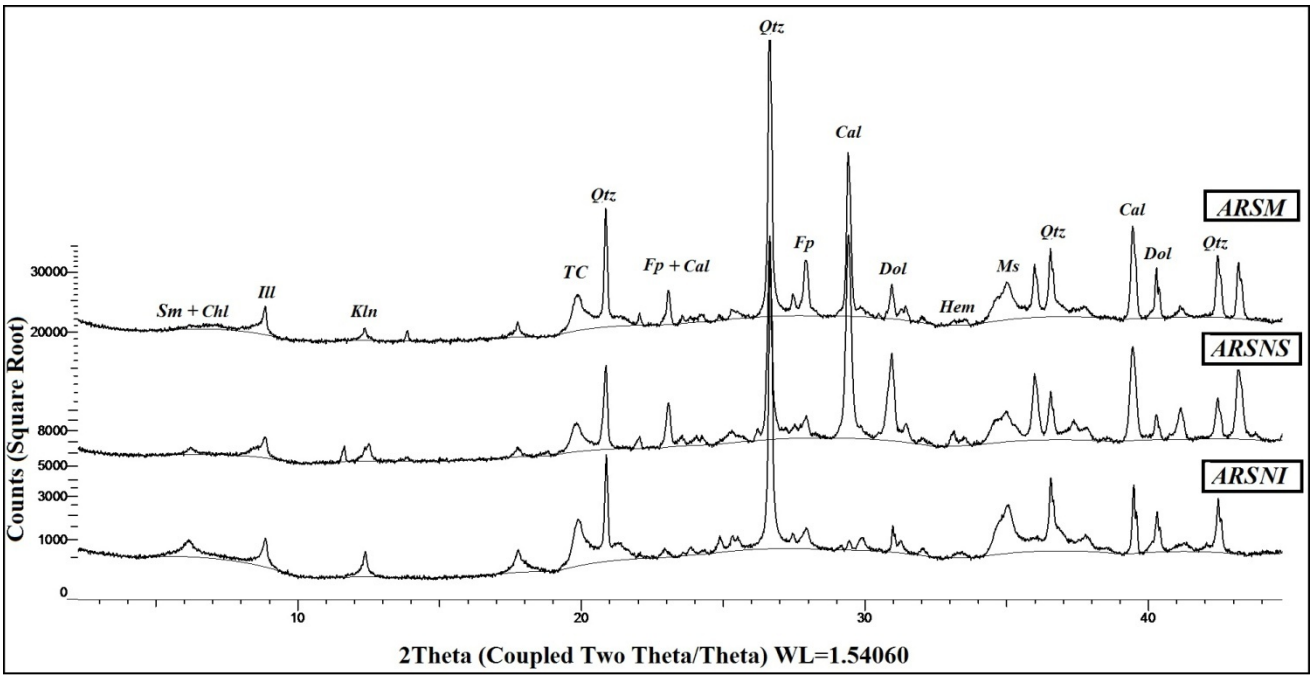

Figure 6: Total mineralogical composition obtained by X-ray diffraction (Qtz: Quartz, Fp: Feldspaths, Cal: Calcite, Dol: Dolomite, Ms: Muscovite, Hem: Hematite, TC: Total clay, Kln: Kaolinite, Sm: Smectite, Chl: Chlorite, Ill: Illite).

These results are complemented by infrared spectroscopy (FTIR), quartz observed by XRD, is confirmed by an intense band between 900 and 1200 cm-1 and centered around 1051 cm-1 corresponding to the stretching vibration of Si-O [15]. Absorption bands located at 872.6 cm^{-1} and 1426,33 cm^{-1} correspond to calcium carbonates $CaCO_3$ [16], these bands are well developed in the ARSM and ARSNS samples. The band observed at 798 cm^{-1} is related to the elongation vibrations of the Si-O-Al bonds [17] and the 663 cm^{-1} band is characteristic of hydroxyl deformation in trioctahedral clay minerals. The peak at 3614 cm^{-1} is attributed to the elongation vibrations of the internal OH groups (Figure 7).

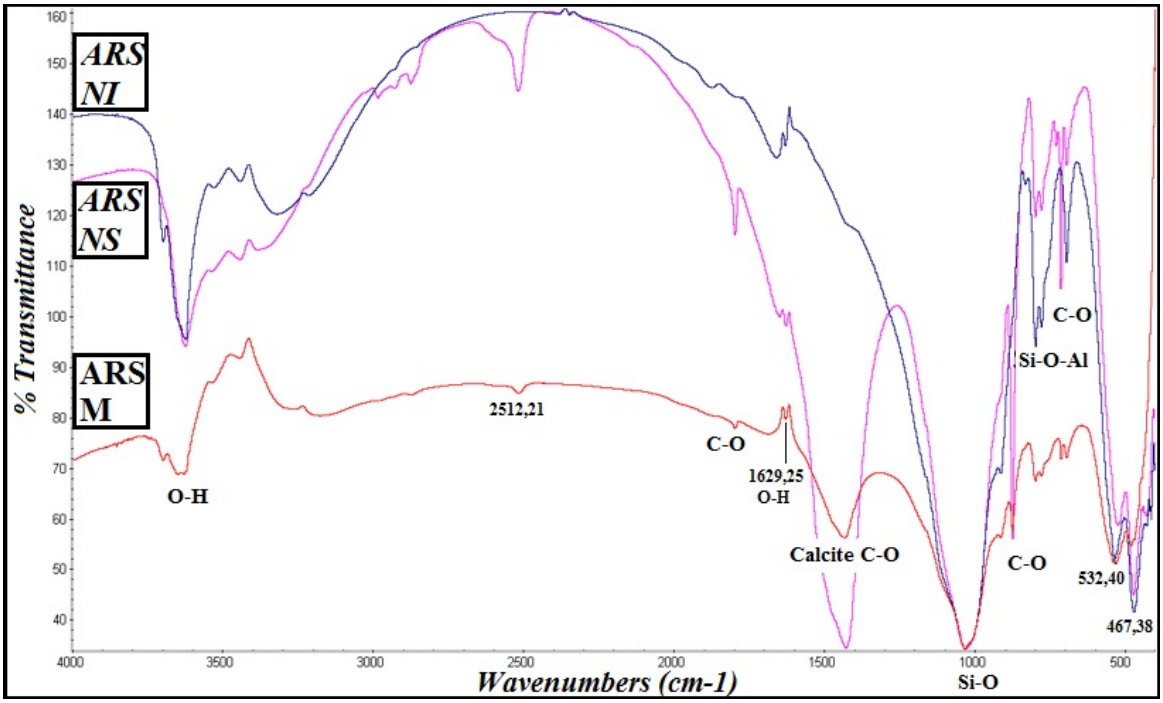

Figure 7: Infrared spectra of the analysed samples obtained by FTIR analysis.

3.1.3. Chemical composition

The most abundant oxides in the three samples are SiO_2, Al_2O_3 and Fe_2O_3, while K_2O, MgO Na_2O, TiO_2 and P_2O_5 are in small amounts except for CaO which is present in high amounts in ARSNS and ARSM samples. The results of the chemical analysis of the major elements are illustrated in the following table.

Table 2: X-ray fluorescence elemental composition (XRF) of the Sale samples

	SiO_2	TiO_2	Al_2O_3	Fe_2O_3	MnO	MgO	CaO	Na_2O	K_2O	P_2O_5	LOI
ARS NI	**56.14**	**0.95**	**17.76**	**6.98**	**0.03**	**1.15**	**0.71**	**0.31**	**2.52**	**0.06**	**13.25**
ARS NS	**36.02**	**0.56**	**8.46**	**3.34**	**0.03**	**3.37**	**20.86**	**0.52**	**1.56**	**0.16**	**23.3**
ARS M	**53.13**	**0.72**	**11.88**	**4.93**	**0.04**	**1.44**	**10.23**	**0.56**	**1.87**	**0.14**	**14.48**

The predominance of oxides SiO_2 and Al_2O_3 is associated to the presence of illite and kaolinite, the mass ratio SiO_2 / Al_2O_3 is 3.2, 4.3 and 4.5 respectively for ARSNI, ARSNS and ARSM indicating the presence of the free quartz in the clay fraction [18]. The Aluminum / Silica ratio can provide information on the moisture permeability of the samples [19]. This ratio is low in all samples and does not exceed 0.31, explaining the low permeability of these materials.

3.1.4. Atterberg limits

Atterberg limits are represented in the diagram of Holtz and Kovacs [20], this diagram shows that the ARSNI sample has a very plastic behaviour (IP = 39.7), whereas ARSNS is considered moderately plastic (IP = 21.9). The mixture of these two samples tends to reduce the plasticity, so the ARSM sample is placed at the boundary between the medium plastic and very plastic field (IP = 27.3) (Figure 8A). The diagram also shows the influence of the nature clay fraction dominates in each sample on its plasticity. In fact, samples whose relatively high on smectite and illite are the most plastic [21].

3.1.5. Thermal behaviour

Thermal analysis allows to observe physico-chemical changes occurring as a function of temperature [22-23]. From 450°C, the clay minerals lose their constitutional water and begin to destruct at 550°C [15]. At this stage, the loss by weight is in the order of 2.5% for ARSNI, 4.4% for ARSNS and 5.5% for ARSM (Figure 8B). Between 600°C and 800°C, carbonate minerals decompose completely [24-25]. The calcite-rich samples show a weight loss about 22.8% for ARSNS and 14.3% for ARSM. While for ARSNI, decomposition of clays generates a weight loss of 9.4% around 800°C. After this temperature, the combination of elements released during firing gives rise to more resistant compounds, and the weight loss becomes stable for the three samples.

3.1.6. Water Absorption

The water absorption test allows to follow the evolution of water retention capacity for each type of sample during cooking (Figure 8C). ARSNI and ARSM samples baked at 1100°C absorb the least amount of water (i.e., having the lowest absorption coefficient). These two samples systematically absorb less water during cooking, with a slower rhythm for ARSM. Until 600°C, there are no major differences in water absorption between the three samples. At 800°C, decomposition of carbonate minerals induces the development of microporosity in the calcite-rich samples, as well as an additional increase in volume, producing microcracks within the structure [26]. This justifies the high-water absorption in this sample between 800°C and 1100°C. While for the ARSNI the absence of carbonate promotes the decrease of porosity in this sample with reduction in connectivity of the pores due to the vitrification.

3.1.7. Evolution of mineralogical composition during cooking

The clay minerals undergo a thermal modification during firing [24, 27], these modifications determine the final properties of the ceramic product. The mineralogical changes observed for each cooking temperature from 500°C to 1100°C differ from one material to another. For non-carbonated sample ARSNI (0.71% CaO), the clay minerals begin to disappear from 550°C to 900°C (Figure 9).

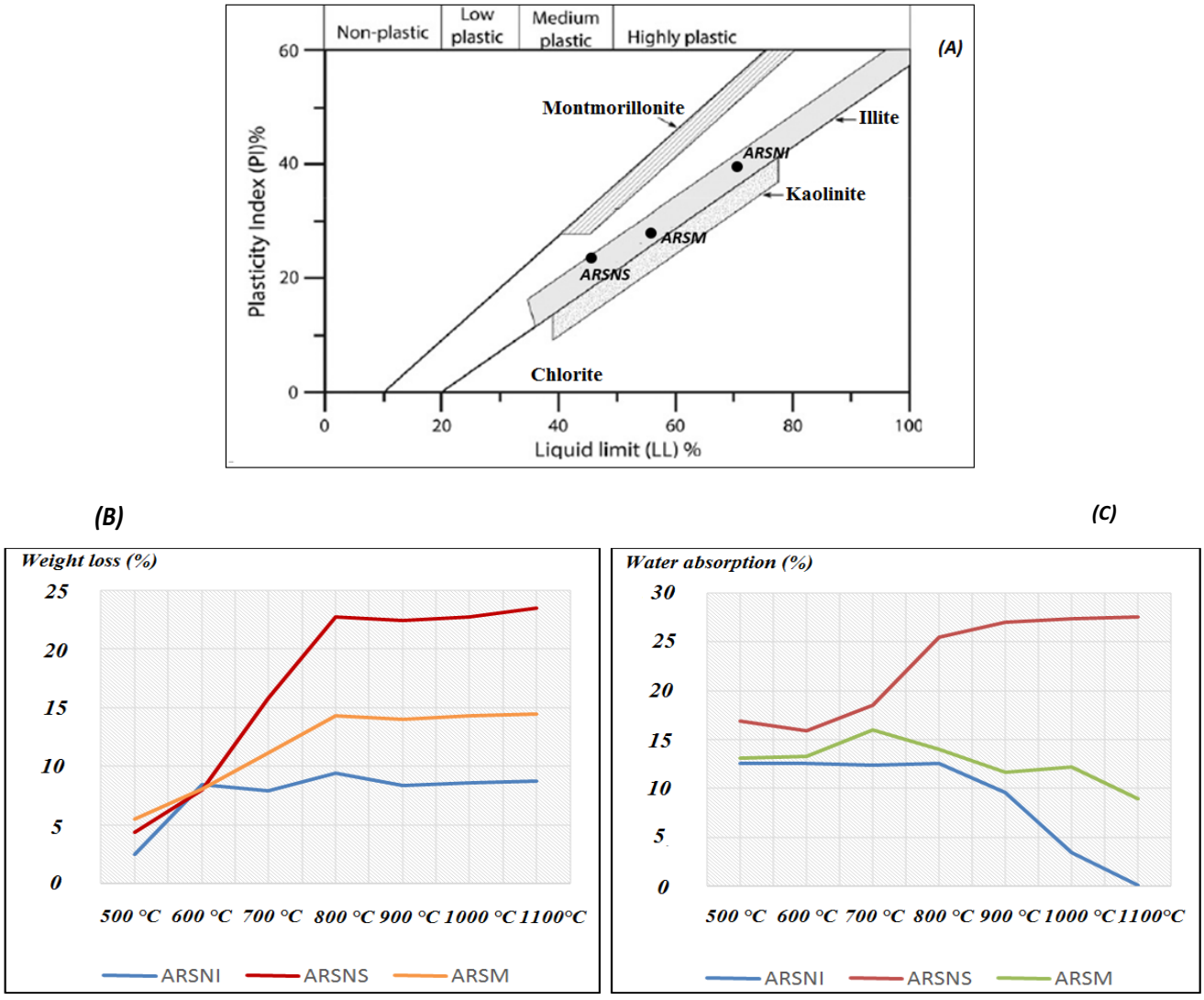

Figure 8: (A) Representation of ARSNI, ARSNS and ARSM samples in the diagram of Holtz and Kovacs [19], (B) The weight loss (in %) and (C) Evolution of the water absorption during cooking (500°C -1100°C).

Plagioclases and muscovite also disappeared close to 950°C. The hematite persists over the entire temperature range and increases proportionally from 900°C, while the peak of the quartz is reduced to half at 1100°C. At this temperature, traces of the mullite begin to appear from aluminium silicate. The spinel derived from dehydroxylation of smectite and chlorite [28] was formed by the reaction $MgO + Al_2O_3 \Rightarrow MgAl_2O_4$. For the rich carbonate sample ARSNS (20.86% CaO), calcite and phyllosilicates disappear respectively at 800°C and 950°C. The first mineral to be formed was gehlenite, which appeared at 800°C, followed by diopside and spinel at 900°C. The peak of hematite increases gradually until reaches a maximum at 1100°C. The presence of small amounts of carbonates inhibited mullite formation, and instead Ca-silicates (gehlenite and diopside) were formed. The mixture sample ARSM shows an intermediate mineral composition at 1100°C, with the peculiarity of appearance of the cristobalite phase at 1000°C.

3.2. Potential of Sale raw material in the ceramic industry

The mineralogical (Figure 10) and chemical (Figure 11) distributions show results comparable to those described in the literature [29]. The ternary diagram based on the DRX results indicates that the two samples ARSNS and ARSNI constitute two distinct poles, the first carbonate rich and the second contains relatively high contents of quartz, feldspars and clay minerals. The mixture of these two materials gives a homogeneous paste suitable for the manufacture of the structural ceramic. The ternary diagram ($Fe_2O_3 + CaO + MgO$ / Al_2O_3 / $Na_2O + K_2O$ is a reference for the classification of clay raw materials used in the ceramic industry. The ARSM sample fits into the red ceramic domain, due to the moderate Fe_2O_3 content, which is about 5% [29-31] and which was contributed by the ARSNI (25% of ARMS).

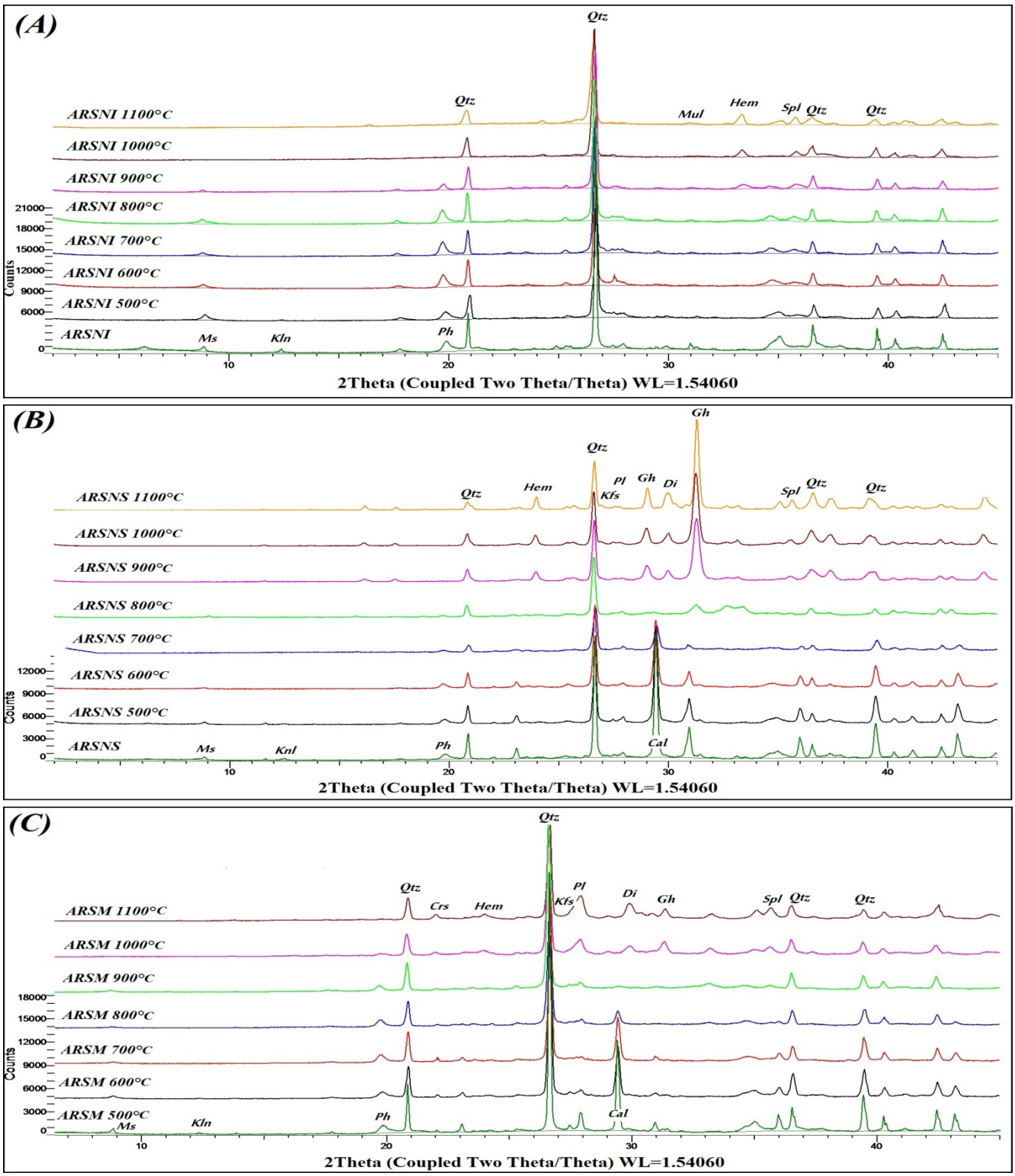

Figure 9: DRX diagrams of ARSNI, ARSNS and ARSM samples at different cooking temperatures. (Ms: Muscovite, Kln: Kaolinite, Ph: Phyllosilictes, Qtz: Quartz, Crs: Cristobalite, Hem: Hematite, Kfs: K-feldspar, Pl: Plagioclase, Di: Diopside, Gh: Gehlenite, Spl: Spinel, Mul: Mullite, Cal: Calcite).

The plasticity of the sample is a prime criterion in the choice of the raw material used in the ceramic industry. The limit of plasticity corresponds to the optimum quantity of water that the clay material acquires to get a plastic consistency, which allows it to be formed by extrusion [6]. Only ARSNS sample is located inside the optimum extrusion zone (Figure 12), the ARSM sample falls into the considered acceptable region, these two samples have an appropriate shaping behaviour [32]. The ARSNI sample exits the acceptable and optimum extrusion zone due to its high plasticity index, suggesting that this clay material is unsuitable for extrusion; it should be mixed with another less plastic material before to be applied in the manufacture of earthen objects.

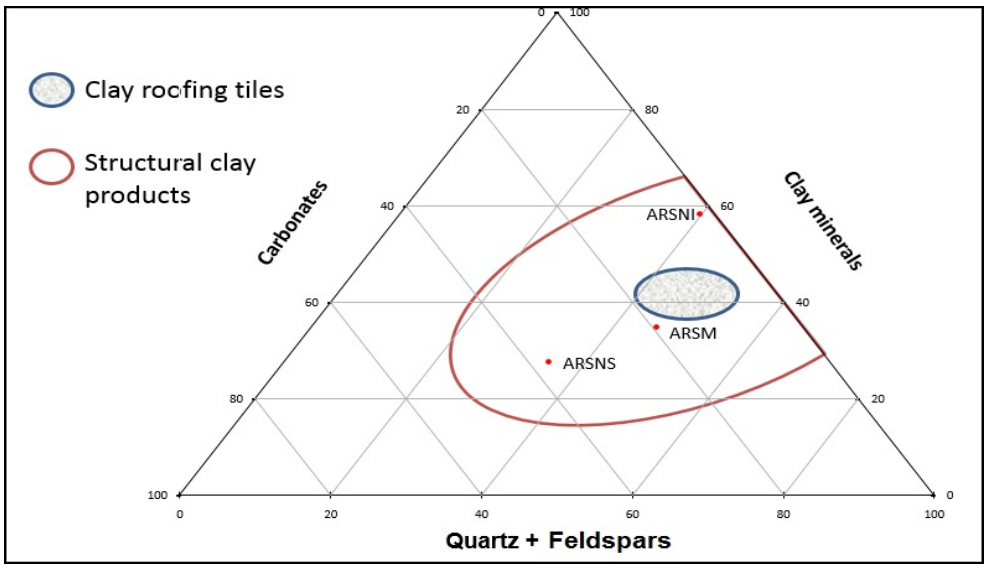

Figure 10: Ternary diagram [29] for the studied samples: Carbonates / Quartz + Feldspars / clay minerals.

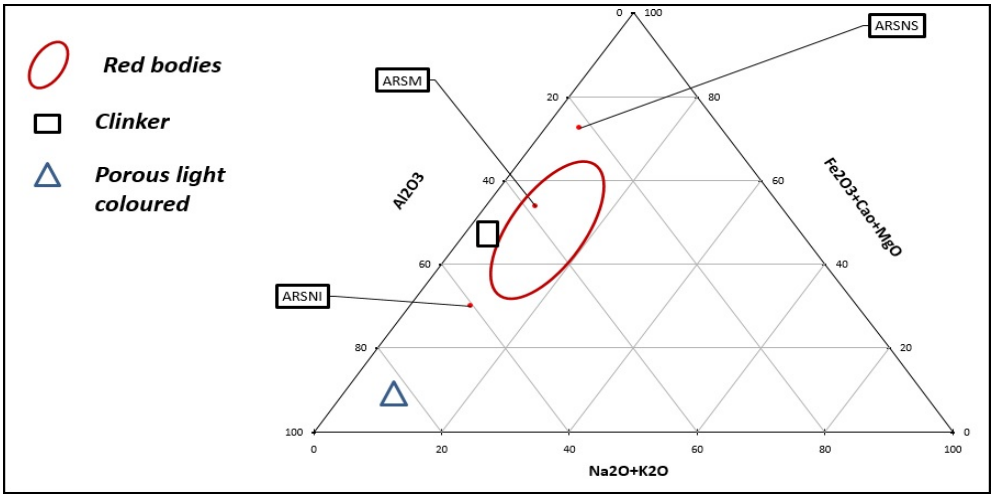

Figure 11: Ternary diagram [29] for the studied samples: Al_2O_3 / Na_2O + K_2O / Fe_2O_3 + CaO + MgO.

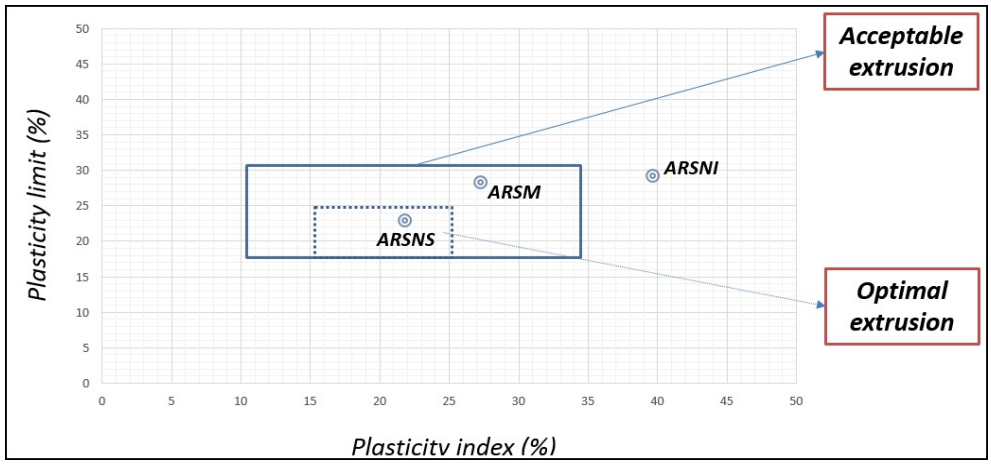

Figure 12: Prognostic Extrusion through the Atterberg boundaries [32]

Conclusion

The chemical and mineralogical analyses carried out on the clay materials used in the Oulja pottery complex show that Oulja clays (ARSNI) cannot be used alone in the ceramic industry because of their high plasticity. The Upper Miocene clays of the Rabat-Sale region (ARSNS) are more suitable for the manufacture of such objects due to their technological properties, but their high $CaCO_3$ content produces a great loss in weight during cooking which causes microcracks in the material and an increase in porosity after cooking. A mixture

between these two materials is then essential to maintain the adequate plasticity of the raw materials and to reduce the effect of decarbonation at high temperature. The ARSM mixture consisting of 75% ARSNS and 25% ARSNI seems to be the most conforming to the requirements of the Oulja potters following their intermediate characteristics and their stabilities during cooking.

Acknowledgements-The financial support is provided by the "Bilateral Cooperation Project Wallonie Bruxelles-Maroc" (Grant 2.7) and by the PPR-CNRST program (Grant PPR1/2015/63) that are all gratefully acknowledged. The first author acknowledges the financial support provided by Erasmus plus.

References

1. M. El Ouahabi, L. Daoudi, F. De Vleeschouwer, R. Bindler, N. Fagel, *J. Min. Mater. Characterization and Engineering*, 2 (2014) 145-159.
2. M. El Ouahabi, L. Daoudi, N. Fagel, *J. Clay Minerals,* 49 (2014) 35-51.
3. B. Achiou, H. El Omari, Bennazha, A. Albizane, L. Daoudi, L. Saadi, M. Ouammou, S. Alami Younssi, A. El Maadi, M. Chehbouni, *J. Mater. Environ. Sci.* 7 (2016) 1474-1484.
4. M. Hajjaji, H. Mezouari, *Appl. Clay Sci*. 51 (2011) 507–510.
5. L. Daoudi, H. Elboudour Elidrissi, L. Saadi, A. Albizane, J. Bennazha, M. Waqif, M. Elouahabi, N. Fagel, *Appl. Clay Sci*.102 (2014) 139-147.
6. H. E. El Boudour, L. Daoudi, M. El Ouahabi, A.B. Madi, F. Collin, N. Fagel, *Appl. Clay Sci.* 129 (2016) 108-115.
7. A. Michard, *Notes et mém. Serv. Géol. Maroc,* 252 (1976) 408.
8. Army geographical service (1936).
9. H.E. Cook, P. D. Johnson, J. C. Matti, I. Zemmels, *In Hayes, D.E., Frakes, L.A., et al., Init. Repts. DSDP, 28: Washington (U.S. Govt. Printing Office)*, (1975) 999-1007.
10. Afnor, NF P 94-068 (1993) 15.
11. Afnor, NF P 94-051 (1993) 95-110.
12. 67-027-84 U. Determinacion de la absorcion de agua de ladrillos de arcilla. Instituto Espanol de Normalizacion, . AENOR. 1984.
13. J. McManus, *Blackwell, Oxford*, (1988) 63–85.
14. Afnor, NF P 94-057 (1992) 157-173.
15. A. Aarfane, A. Salhi, M. El Krati, S. Tahiri, M. Monkade, E.K. Lhadi, M. Bensitel, *J. Mater. Environ. Sci.* 5 (2014) 1928.
16. A. Lahsini, J. Bentama, A. Addaou, M, Rafiq, *J. Chim. Phys*. 95 (1998) 1001.
17. K. L. Konan, J. Soro, J.Y.Y. Andji, S. Oyetola, G. Kra, *J. Soc. Ouest-Afr. Chim*. 30 (2010) 29.
18. A. Besq, C. Malfoy, A. Pantet, P. Monnet, D.Righi, *Appl. Clay Sci*. 23 (2003) 275-286.
19. I. Jarraya, S. Fourmentin, M. Benzina, *J. Soc. Chim. Tunisie*, 12 (2010) 139-149.
20. R.D. Holtz, W.D. Kovacs, *Prentice-Hall, Inc., New Jersey*, (1981) 747.
21. W. Hajjaji, M. Hachani, B. Moussi, K. Jeridi, M. Medhioub, A. López-Galindo, F. Rocha, J.A. Labrincha, F. Jamoussi, *J. Afr. Earth. Sci*. 57 (2010) 41-46.
22. F. Sahnoune, M. Chegaar, N. Saheb, P. Goeuriot, F. Valdivieso, *Appl. Clay Sci*, 38 (2008) 304-310.
23. F. Hubert, L. Caner, A. Meunier, B. Lanson, *Eur. J. of Soil Sci*, 60 (2009) 1093-1105.
24. G. Cultrone, C. Rodriguez-Navarro, E. Sebastian, O. Cazalla, M.J.D.L. Torre, *Eur. J. of Mineralogy*, 13 (2001) 621-634.
25. G. Périnet, L. Courtois, *Bull. Soc. préhistorique française*, 80-5 (1983) 157-160.
26. G. Cultrone, E. Sebastian, K. Elerta, M.J. De la Torre, O. Cazalla, C. Rodriguez–Navarro, *J. Eur. Ceramic Society*, 24 (2004) 547–564.
27. M.M. Jordan, T. Sanfeliu, C. De la Fuente, *Appl. Clay Sci*, 20 (2001) 87-95.
28. M. El Ouahabi, L. Daoudi, F. Hatert, N. Fagel*, Clays and Clay Minerals,* 63-5 (2014) 404-413.
29. C. Fiori, B.Fabbri, G. Donati, I. Venturi, *Appl. Clay Sci*, 4 (1989) 461–473.
30. H.H. Murray, *Appl.clay mineralogy. Elsevier B.V*, 2 (2007) 180.
31. H. Baccour, M. Medhioub, F. Jamoussi, T. Mhiri, A. Daoud, *Mater. Charact*, 59 (2008) 1613–1622.
32. M. Marsigli, M. Dondi, *L'industria Laterizi*, 46 (1997) 214–222.